



Single molecule unfolding and stretching of protein domains inside a solid-state nanopore by electric field

SUBJECT AREAS:

NANOSCALE
BIOPHYSICS

CONFORMATION

DEFORMATION DYNAMICS

NANOPORES

Kevin J. Freedman¹, S. Raza Haq², Joshua B. Edel³, Per Jemth² & Min Jun Kim⁴

¹Department of Chemical and Biological Engineering, Drexel University, Philadelphia, Pa 19104, USA, ²Department of Medical Biochemistry and Microbiology, Uppsala University, Uppsala, Sweden, ³Department of Chemistry, Imperial College London, South Kensington, SW7 2AZ, London, United Kingdom, ⁴Department of Mechanical Engineering and Mechanics, Drexel University, Philadelphia, PA 19104, USA.

Received
6 November 2012

Accepted
22 March 2013

Published
10 April 2013

Correspondence and
requests for materials
should be addressed to
M.J.K. (mkim@coe.
drexel.edu)

Single molecule methods have provided a significantly new look at the behavior of biomolecules in both equilibrium and non-equilibrium conditions. Most notable are the stretching experiments performed by atomic force microscopes and laser tweezers. Here we present an alternative single molecule method that can unfold a protein domain, observed at electric fields greater than 10^6 V/m, and is fully controllable by the application of increasing voltages across the membrane of the pore. Furthermore this unfolding mechanism is characterized by measuring both the residence time of the protein within the nanopore and the current blockade. The unfolding data supports a gradual unfolding mechanism rather than the cooperative transition observed by classical urea denaturation experiments. Lastly it is shown that the voltage-mediated unfolding is a function of the stability of the protein by comparing two mutationally destabilized variants of the protein.

The folding of a linear amino acid sequence into a three dimensional structure is a crucial process in biology that yields a particular functional form of the protein¹. Due to the vast number of degrees of freedom of the polypeptide chain, folding is currently understood to occur on a complex energy landscape which directs the protein to the singular native state (i.e. the energy minimum)²⁻⁵. However a complete understanding of the process has yet to be achieved stemming from the interplay of a large number of interactions⁶⁻⁹. A fundamental problem involved with studying protein folding is that it is extremely difficult to characterize all states, i.e. the conformational ensemble, for a given protein¹⁰⁻¹². The reason for this is partly due to the small energy differences between states leading to folding transitions that occur on extremely small timescales¹³. Experimental techniques that are capable of sampling from the conformational space and explore regions of the energy landscape that are not accessible in bulk are particularly useful for addressing this problem⁶.

Single molecule methods have aimed to solve this problem by manipulating proteins under non-equilibrium conditions while simultaneously measuring single molecule properties^{6,14-17}. Despite advances in NMR which can now resolve low-populated protein states¹⁸, the ability to unfold proteins as well as measure single molecule information is extremely powerful for characterizing uncharted regions of conformational space. This has been most notably achieved using an atomic force microscope in which proteins have been stretched in order to characterize folding forces^{6,15}. In terms of high-throughput analysis of molecules, however, nanopores have several unique attributes when it comes to single molecule sensing. One of these is the ability to measure the volume of a molecule which provides information on molecular size and shape and solvent-solute interactions. The second property can additionally provide indirect information about surface charge by the translocation time as well as the effective increase in size due to bound ions which screen charged regions of the molecule^{19,20}. The first property however is most advantageous for studying protein folding. A series of experiments have demonstrated the ability of nanopores to discriminate between conformations of DNA²¹ as well proteins with and without a denaturant²²⁻²⁸. Characterization of a single molecule's unfolded state is also a unique attribute of nanopores since most bulk measurements cannot accurately describe the multitude of sub populations of states. The non-equilibrium condition that nanopores provide is the necessary electrical force that drives the protein across the membrane and through the single nanopore drilled in it. Since the majority of the applied voltage drops across the pore, when the protein approaches the pore entrance, it begins to experience an electric field



proportional to the driving voltage (Fig. 1c). Due to the heterogeneous charge of the molecule, as well as the existence of a net dipole moment, the electric field has been speculated to induce local or global unfolding of proteins^{23,28}.

The nanopore technique allows one to probe the conformational space of proteins. Several studies with protein channels or solid-state nanopores have been able to detect the unfolding process^{22–28} with some experiments even generating unfolding curves of wild type and/or mutant proteins using event frequency analysis^{24,26,27}. In regard to studying the effects of the electric field, Pelta and colleagues²⁵ have investigated the translocation dynamics of the folded and completely unfolded states within the range of 50–250 mV for maltose binding protein. Within the 50–250 mV regime, they demonstrated that the folded state behaves as expected for a particle that does not change shape; namely that the amount of current blocked by the protein increases linearly with voltage and translocation time decreases with voltage. For the conformationally dynamic unfolded state, they found a slight reduction in the excluded volume leading to a protein stretching hypothesis. Further study by the same group confirmed the stretching hypothesis for the unfolded protein by showing that the normalized current blockage decreases up to 400 mV and becomes constant between 400 to 800 mV suggesting above 400 mV the denatured protein is fully extended inside the narrow pore diameter²². The question we aim to answer is whether elevated electric fields can unfold conformationally stable proteins and what conformations do the proteins assume within the pore. In the current work we characterize the changes in residence time within the pore, current drop due to the protein, and the excluded volume of the protein as a function of applied voltage. Importantly, we perform these experiments with three variants of a protein domain, SAP97 PDZ2, each having distinct free energies of

unfolding, ΔG_{D-N} . We show that the electric field within the pore can denature the proteins and be used to obtain a relative measure of stability. Therefore this represents a new approach to unfold proteins that can controllably manipulate the folding of a single protein within a localized region.

The protein that we are studying, SAP97 PDZ2, is a member of a ubiquitous protein domain family (PDZ) found within many organisms and in a few hundred proteins in humans²⁹. It acts as a modular interaction domain that participates in holding together protein assemblies involved in signaling and subcellular transport^{30,31}. Disruption of PDZ containing proteins through mutation has been implicated in several human diseases. These include Usher syndrome, cancer, cystic fibrosis, Parkinson's disease, and chronic kidney disease^{32–34}. It is a relatively small protein domain ($\sim 4 \times 5$ nm) with a low net positive charge (+3.8 e) at neutral pH. The 109 amino acid sequence leads to an approximate contour length of 42 nm which even in its linear form would fit within the pore. Therefore all conformations can be probed without having to speculate about whether portions of the protein are outside the pore and, as a result, not being sensed. Using the SAP97 PDZ2 and two site-directed mutants we characterized the folded as well as the chemically denatured state and found that both become further unfolded in the presence of an electric field.

Results

Competing Denaturation: Urea versus Electric field. The work of Talaga and Li²⁸ demonstrated the ability of solid-state nanopores to discriminate between conformational states of a protein under three different urea concentrations. Here we used protein solutions with no urea and 8 M urea and performed a comparative study of the changes between the native and unfolded state over a range of voltages (200–800 mV). Through these experiments we intend to study several biophysical events: firstly, detect any changes in structure caused by the chemical denaturant urea, secondly, determine if the unfolded, flexible protein state changes as a function of voltage, and thirdly, determine if the native, stable protein state becomes unfolded at voltages above 200 mV. The protein analytes used in this work are three different forms of the SAP97 PDZ2 domain; specifically the I342W/C378A double mutant referred to as the wild type³⁵, V388A and L322A (both also having the I342W/C378A mutations). The folding of all three SAP97 PDZ2 domains involves an intermediate but is best described as being two state in equilibrium denaturation experiments^{36,37}. The V388A and L322A mutations are destabilizing such that the change in global free energy of unfolding, $\Delta\Delta G_{D-N}$ upon mutation were estimated to be 0.6 and 3.3 kcal mol⁻¹, for V388A and L322A, respectively, as determined from urea denaturation experiments at equilibrium (Supporting Information).

Using the V388A form of the protein domain, which has the closest stability to proteins used in previous works^{23,28,38,39}, the dynamics of the current drop were investigated as a function of voltage. The expectation would be that if the conformation of the protein (either folded or unfolded) was not changing within the pore, the current drop should increase linearly with voltage. Such behavior has been shown most recently by experiment²⁵ as well as with simulations (Supporting Information). The observed trend in current drop however showed non-linear behavior over the range of voltages tested (Fig. 2a). At 200 mV, the absolute value of the current drop for 0 M and 8 M urea were 915 ± 10 pA ($n = 1719$) and 965 ± 40 pA ($n = 992$), respectively. It should be noted that the increase in current drop upon adding urea corresponds to an even larger change in excluded volume since the conductivity of the solution is reduced upon adding urea. At 300 mV, the absolute value of the current drop for 0 M and 8 M urea were 928 ± 17 pA ($n = 703$) and 966 ± 46 pA ($n = 1635$), respectively. If we assume that the protein does not deform significantly across voltages, the current drop should roughly

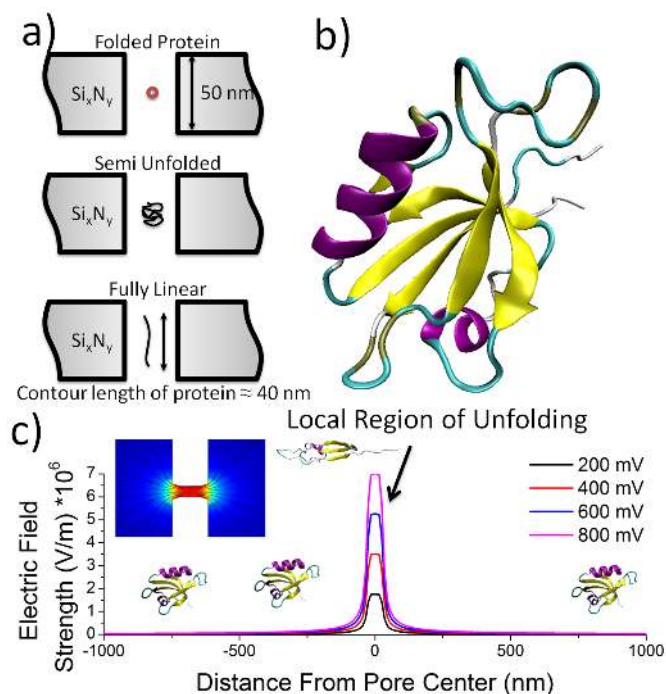


Figure 1 | (a) Schematic showing the expected protein states in relation to the principal sensing element, a 15 nm solid-state nanopore, drilled in a 50 nm thick silicon nitride membrane. (b) Crystal structure for the SAP97 PDZ2 domain. PDB CODE: 2X7Z. (c) Finite element simulations showing the electric field plotted as a function of distance from pore center; pore dimensions: 15 nm diameter, 50 nm thick membrane. This was performed over the range of 200–800 mV in which the effects on protein folding are investigated.

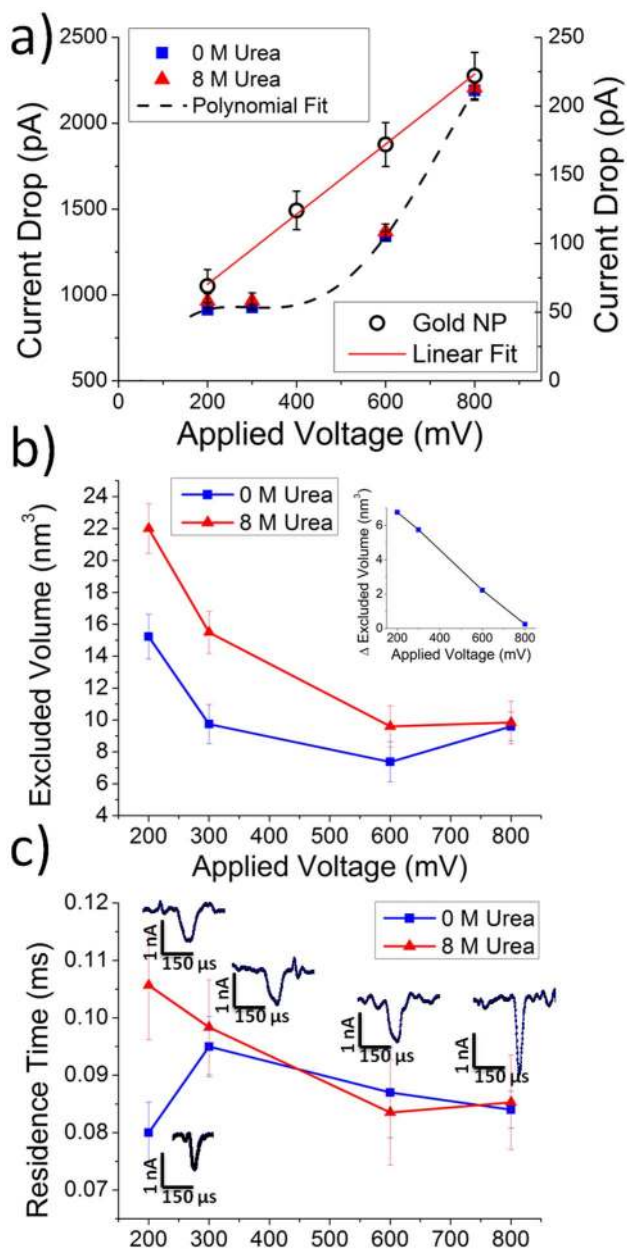


Figure 2 | (a) Current drop parameter plotted as a function of applied voltage with and without urea for the V388A SAP97 PDZ2 domain. Also plotted (right axis) is translocation data for a stable fixed-shape particle (5 nm gold nanoparticles: gold NP) showing a linear dependence with voltage (see Supporting Information for event statistics). (b) Residence time plotted as a function of applied voltage for protein samples with and without urea. Insets: characteristic event traces for corresponding applied voltages at 0 M urea. Residence time histograms are available in the Supporting Information. (c) Calculated excluded volume parameter as a function of applied voltage with and without urea. Insets: the change in excluded volume between the samples with urea and without urea. The experiments were performed in 2 M KCl and 10 mM potassium phosphate buffer (pH 7). Data was collected with the same 15 nm pore at 200 mV ($n_{0M} = 1719$, $n_{8M} = 992$), 300 mV ($n_{0M} = 703$, $n_{8M} = 1635$), 600 mV ($n_{0M} = 768$, $n_{8M} = 1968$), and 800 mV ($n_{0M} = 1493$, $n_{8M} = 5604$).

scale with voltage and therefore the values at 300 mV should be 1.5 times those at 200 mV. Instead at 0 M and 8 M urea, the current drop is identical, within error. On the other hand, the current drop between 600 mV and 800 mV showed an increase of 1.63 and

1.61 times for 0 M and 8 M urea, respectively, when it would be expected to be 1.3 (i.e. 800/600). This behavior in the current drop suggests that the protein is changing its folding as the applied voltage is increased.

The curve that best fits the dynamics of the current drop, and thus describes unfolding behavior, is shown to be a cubic polynomial which was chosen arbitrarily according to least error. We expect this curve to be valid within the range of voltages that unfolding takes place. At voltages at or below 200 mV we expect that the protein is stable and thus current drop would be linearly dependent with voltage, as shown by Oukhaled et al.²⁵. We can further assume that the current drop will regain a proper scaling behavior when the protein is fully unfolded; however for the more stable domains this linear regime is believed to be above the maximum applied voltage allowed by the recording system. Given that a stable protein conformation yields a linear dependence with applied voltage, the mathematical function describing the current drop as a function of voltage seems to be a piecewise function where linearity is interrupted only when protein unfolding is occurring. The linear dependence of a stable particle going through a nanopore of the same size was confirmed in a control experiment using 5 nm gold nanoparticles at a reduced electrolyte concentration (0.2 M KCl) to avoid aggregation (Fig. 2a, see Supporting Information for event histograms).

In order to obtain size estimates for each protein state we used the equation for the excluded volume of electrolyte inside the pore given by: $\Lambda = \Delta I_B H_{eff}^2 / \sigma V$ where ΔI_B is the ionic current blockade amplitude, H_{eff} is the effective length of the pore, σ is the conductivity of the electrolyte, and V is the applied voltage. Despite the literature giving a value to H_{eff} based on the thickness of the membrane, we have found this led to significant error in the calculation. Since H_{eff} is in the equation as an approximation of the electric field (V/H_{eff}) which also significantly depends on the diameter of the pore, this is rarely an accurate assumption that should be used. Here, we use the same H_{eff} throughout (see Supporting Information for justification for keeping H_{eff} constant). The magnitude was found by solving for the known volume of the folded state ($\sim 17 \text{ nm}^3$) which gave a H_{eff} value of 9 nm. Also, since excluded volume is dependent on the shape of the molecule which we do not know in this case we use variations in excluded volume to indicate shape changes. Therefore, implicit in the above equation is a shape factor of 1^{40,41}.

The current drop value alone was observed to increase when 8 M urea was present (at 200 mV: $915 \pm 10 \text{ pA}$ ($n = 1719$) and $965 \pm 40 \text{ pA}$ ($n = 992$); although difficult to see in Fig. 2a) however this increase represents an even larger increase in size due to the reduced conductivity of the solution upon adding urea (205 mS/cm and 158 mS/cm for 0 M and 8 M, respectively). As initially expected based on previous results²³, the protein sample with urea has a larger excluded volume compared to the no urea sample particularly at lower applied voltages (Fig. 2b). The second observation is that the urea-induced increase in excluded volume is reduced as voltage is increased (Fig. 2b inset) indicating the folded and unfolded protein are blocking more similar currents at higher voltages. The fact that unfolded proteins will block a lower fraction of current due to stretching was already confirmed²² however in this case both protein states converge to produce similar electrical signals irrespective of the presence of urea.

Since 8 M urea usually completely unfold proteins⁴² including SAP97 PDZ2³⁵, the changes in excluded volumes that are seen in the protein with urea, we hypothesize, are due to a folding force not related to intra-protein interactions but rather the conformational entropy of the unfolded protein chain⁴³. There are two ways in which conformational entropy is low: when the protein is tightly packed into its native state and when the chain is linear which also highly restricts chain movements⁴³. As the flexible protein chain enters the pore, we expect that the electric field causes the positive and negatively charged amino acids to align with the field



and therefore overcomes the second form of conformational entropy. Most interestingly, the protein without urea obtains this same excluded volume suggesting that the electric field is capable of overcoming both the interaction forces within the protein as well as the conformational entropy force which both find the linear conformation energetically unfavorable. Given this interpretation, we can see that the protein with urea reaches this linear state at 600 mV whereas the protein without urea requires a greater force to overcome the interaction energies between residues.

It should be noted that the excluded volume values that we obtain are purely useful in understanding how the measurement changes in response to protein unfolding while making no explicit assumptions about the shape of the molecule. These changes can then be further investigated through the mapping of various shape transformations computationally and correlating them to how the protein changes within the pore. Briefly, this was performed by considering an axial symmetric particle of radius r_p and length l_p submerged in an electrolyte solution that was able to change shape while keeping a constant occluding area within the pore. Two state models did not explain the observed trends we saw experimentally and inevitably led to a two state excluded volume curve (Supporting Information). However, using a particle with a constant occluding area of 36 nm^2 that gradually elongated in length from $6 \times 6 \text{ nm}$ (roughly the long axis of a fully folded SAP97 PDZ2 molecule) to $1 \times 36 \text{ nm}$ (roughly the length of the fully linear SAP97 PDZ2 molecule), the observed trend agrees with the experimentally observed changes in excluded volume. From this analysis we observed how various parameters such as molecular width and length affected the ionic current through the pore. Thus, a general conclusion of this work is that changes in excluded volume can be used to identify changes in structure of the protein. However as the aspect ratio of the protein becomes large ($3 \times 12 \text{ nm}$ in this study), the excluded volume is not specific to a single structure.

The residence time (i.e. time to translocate the pore) was similarly plotted over the same applied voltages (Fig. 2c). If we once again assume a protein which does not significantly deform across voltages, we would expect that the translocation time would decrease exponentially with voltage as observed with folded proteins²⁵. The exponential dependence is a characteristic of a free energy barrier to the translocation process which has been observed previously with proteins translocating both biological and solid-state pores^{25,44,45}. Given our nanopores have a smaller diameter and larger membrane thickness than previous reports²⁵, the energy barrier will most definitely govern translocation kinetics. Nevertheless, the observed curve for the folded state (Fig. 2c) does not agree with the expected exponential dependence characteristic of previous experiments²⁵. The 8 M urea curve follows a qualitative exponential reduction in residence time consistent with what we would expect assuming barrier-dominant translocation theory. Interestingly, between 200 mV and 300 mV, the protein without urea significantly increases its residence time despite the electrophoretic force being increased. Also, it obtains a residence time that matches more closely to that of the unfolded protein. Above 300 mV, the sample without urea present continues the trend observed for the 8 M urea protein sample. This initially suggests that the application of a mid-level voltage ($\sim 300 \text{ mV}$) causes a change in protein migration through the pore likely stemming from a change in protein conformation. It should be noted that slower migration speeds of the unfolded state of a protein compared to the folded form has been observed with capillary electrophoresis⁴⁶. In these experiments, a slower migration speed was due to a high-to-low transition in the protein's electrophoretic mobility upon unfolding stemming from an increase in the protein's hydrodynamic radius commonly linked to unfolding^{23,46}.

It should be noted that the observed residence times are significantly longer than expected for our experimental conditions. The electrophoretic velocity of a protein in an electric field is given by:

$$V_p = \frac{q_p E}{6\pi\eta r_p}$$
 where q_p is the net charge of the protein, r_p is the protein radius, η is the viscosity of the solution, and E is the electric field strength. Given the high aspect ratio of the pore, we can assume that the recorded residence time, τ_{ele} , can be approximated by $\tau_{ele} = \frac{L_{pore}}{V_p}$ and that the electric field by $E = \frac{V_{applied}}{L_{pore}}$. Using $q_p = +3.8e$, $r_p = 2 \text{ nm}$, $L_{pore} = 50 \text{ nm}$, $\eta = 10^{-3} \text{ Pa s}$, $V = 200 \text{ mV}$, the theoretical residence time can be calculated to be $0.73 \mu\text{s}$. Assuming no voltage and simply diffusion, the residence time would be $\tau_{diff} = \frac{6\pi\eta r_p L^2}{k_B T} = 22 \mu\text{s}$.

Given the fact that we observe residence times much greater than these values even when assuming no driving force, there are likely transient interactions between the pore and the protein occurring throughout the translocation process that slows down the protein. A second hypothesis that has been previously proposed includes taking into account electroosmotic flow which can potentially slow the protein's migration through the pore⁴⁷. However in the experiments presented here, the electroosmotic flow is in the same direction as the applied voltage force leaving either interactions or an entropic exit barrier being possible causes for the long events^{48,49}.

Interactions were ruled out as causing adsorption-induced unfolding for several reasons. First, previous studies with folded proteins observed even larger residence times and yet no evidence of unfolding as observed here²⁵. Secondly, the changes in residence times were minor across voltages compared to the large changes in excluded volume. Finally, longer residence times were not consistent with a small excluded volume as might be expected (e.g., the largest residence time was obtained for the 8 M urea condition at 200 mV which, if unfolded and adsorbed to the pore, should block the least amount of ion flow however this condition yielded the highest excluded volume).

Protein stability effects on residence time and excluded volume.

Residence time kinetics were obtained over the same range of voltages (200–800 mV) for the wild type SAP97 PDZ2, a mildly destabilized (V388A), and a highly destabilized variant (L322A). Interestingly, increases in residence time despite larger voltages being applied to the nanopore are observed for each of the three PDZ2 domains (Fig. 3a). Such increases in residence time can only be explained by unfolding since translocation theory and previous work with DNA and proteins show a decrease in residence time with increasing voltage^{22,25,50}. Although a gradual change in structure has been outlined, there seems to be a characteristic voltage where unfolding causes an anomalous increase in residence time. This is observed in each SAP97 PDZ2 variant at a different voltage. For wild type SAP97 PDZ2 (i.e. the most stable domain), the voltage in which the protein begins to decrease its residence time in comparison to lower voltages occurs at 800 mV. For the two destabilized mutants, this occurs at 600 mV suggesting that there is a voltage-dependent transformation that affects residence time.

As discussed earlier, the anomalously long residence times observed in these experiments suggests interactions between the pore and the protein^{48,51}. It should be noted once again that this holds true for all three domains under the driving voltages tested here. Therefore, the residence time is not simply a measure of the electrophoretic mobility. However, both the electrophoretic mobility and the number of interactions with the pore are expected to change due to the unfolding of the domains; particularly given that unfolding can expose new residues that were hidden in the original folded molecule. Given the near identical size and sequence of the domains, the observed changes in residence time can be interpreted as being solely dictated by whether or not unfolding occurs. If we take this approach and look only at the data at 200 mV, the data most strongly correlates with the degree of unfolding based on the known stabilities of each domain (i.e. the most stable has the shortest residence time and the

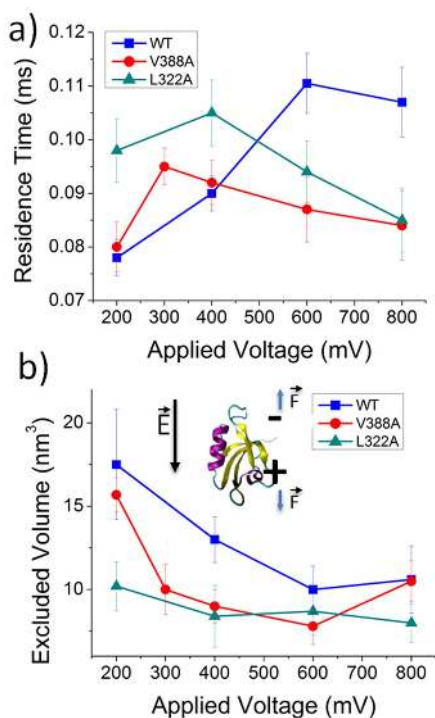


Figure 3 | (a) Residence time as a function of applied voltage for three SAP97 PDZ2 domains with varying stabilities (wild type (WT) SAP97 PDZ2 > V388A > L322A). (b) Excluded volumes as a function of voltage for the same three SAP97 PDZ2 domain variants. The domains were diluted in 2 M KCl and 10 mM potassium phosphate buffer (pH 7). Data was collected with pores 15 ± 2 nm in diameter for the I342W domain ($n_{200\text{mV}} = 202$, $n_{400\text{mV}} = 1005$, $n_{600\text{mV}} = 1474$, $n_{800\text{mV}} = 1006$), the V388A domain ($n_{200\text{mV}} = 1719$, $n_{300\text{mV}} = 703$, $n_{600\text{mV}} = 768$, $n_{800\text{mV}} = 1493$), and the L322A domain ($n_{200\text{mV}} = 233$, $n_{400\text{mV}} = 674$, $n_{600\text{mV}} = 607$, $n_{800\text{mV}} = 550$).

most unstable has the slowest residence time). Increasing residence time with decreasing stability can be explained by the unfolding of the domains by a corresponding reduction in electrophoretic mobility (caused by an increase in hydrodynamic diameter). The second trend observed in Figure 3a is that above 300 mV only the destabilized mutants seem to have a decreased residence time with increased driving force while the most stable domain, we believe, continues unfolding as voltage is increased. All three domains at some point within the voltage range of 200–800 mV increase in residence time despite increasing electrophoretic force which is not consistent with previous data assuming static protein conformations²⁵. It should also be kept in mind that potentially opposing forces such as electroosmotic flow are in the same direction as the electrophoretic force.

The evidence for stability-dependent translocation kinetics between the mutants is further supported in light of calculating excluded volumes. When comparing the wild type SAP97 PDZ2 and the V388A mutant, we observe a very similar trend in which the excluded volume measure progressively decreases between 200 and 600 mV (Fig. 3b). It is most noteworthy that the V388A mutant shows a more prominent decrease at lower voltages. At the highest voltage, nevertheless, both protein domains obtain a common unfolded state. The V388A domain starts out at a lower excluded volume (at 200 mV) and decreases more readily than wild type SAP97 PDZ2 suggesting a greater propensity to electric field-induced unfolding. The most destabilized domain has the smallest excluded volume at 200 mV indicating it is most affected by the electric field. As the voltage is increased further, this domain does not make any significant changes in excluded volume suggesting it is fully unfolded

at low voltage while the more stable domains are still undergoing voltage-mediated unfolding.

Excluded volumes and stability measurement. Since information was collected on each individual molecule, it is possible to calculate the number of proteins that populate the native state and compare this to the total number of proteins. Here we defined the natively folded state using a set of boundaries along the excluded volume axis. Due to the high sensitivity of current drop and excluded volume on the width parameter of the molecule, the initial deviation from the actual folded state is expected to be well discriminated from all the possible non-native states. To define the boundaries, a Gaussian distribution was fitted to the wild type SAP97 PDZ2 data at 200 mV where the highest population of the folded state is expected. Using the full width half max of the distribution we defined the folded state as having an excluded volume between the values of 14 nm³ and 21 nm³ (Fig. 4). Subsequent classification of each translocation event could then be performed as being folded or unfolded. The free energy change accompanying the conformational unfolding induced by the electric field was calculated using: $\Delta G_{D-N} = -RT \ln(K_{eq})$ where K_{eq} is the fraction of folded molecules.

Shifts from this defined natively folded state led to a decreased fraction of folded versus unfolded molecules and therefore to a lower free energy (Fig. 5). When comparing the PDZ variants, we see a qualitative agreement with the known stabilities for each domain. The V388A mutant shows a drastic shift to lower excluded volumes and at a lower voltage (Fig. 4) compared to the wild type SAP97 PDZ2 domain leading to a drop in stability (Fig. 5). As voltage is increased further the native state of SAP97 PDZ2 continues losing stability until it finally reaches a point in which neither the wild type nor the V388A mutant can be unfolded any further. The L322A mutant even at the low voltages is out of range for being classified as folded and this leads to a lower free energy. Interestingly, the nanopore method of quantifying the fraction of unfolded proteins matched extremely well with bulk stability measurements when comparing relative stabilities calculated from urea-induced denaturation experiments (performed using fluorimetry) and 400 mV (nanopore method) for the three domains (Fig. 6). The slope of the line when comparing the two methods was 1.08 which indicates a strong agreement between the two methods. The concentration which yielded the strongest correlation was 3.1 M urea which suggests that 400 mV has a denaturing effect that is comparative to that of urea at this concentration.

Discussion

In this work we have demonstrated a new method of single molecule protein unfolding in which one can both denature and measure properties of the resulting protein state (i.e. overall shape and migration speed through a nanopore). This method requires no special protein preparation other than having a purified sample and can be conducted in a high throughput manner. Of particular interest, this method of protein analysis was performed using a single solution (per analyte) and by applying various electric potentials. The information obtained from these methods represent a unique look into the behavior of proteins within a pore biased with a voltage. We investigated various parameters such as the current drop, residence time, and calculated excluded volumes and interpreted these changes in terms of structural changes within the nanopore. In doing this, we discovered that the unfolding pathway is not a two-state, cooperative system but rather a gradual deformation or stretching of the protein along the axis of the electric field. Finally, we calculated the changes in free energy associated with these conformational changes. These techniques represent a novel paradigm to study protein folding as well as a method to obtain important biophysical information such as relative stability within a nanopore, which correlates with overall thermodynamic stability.

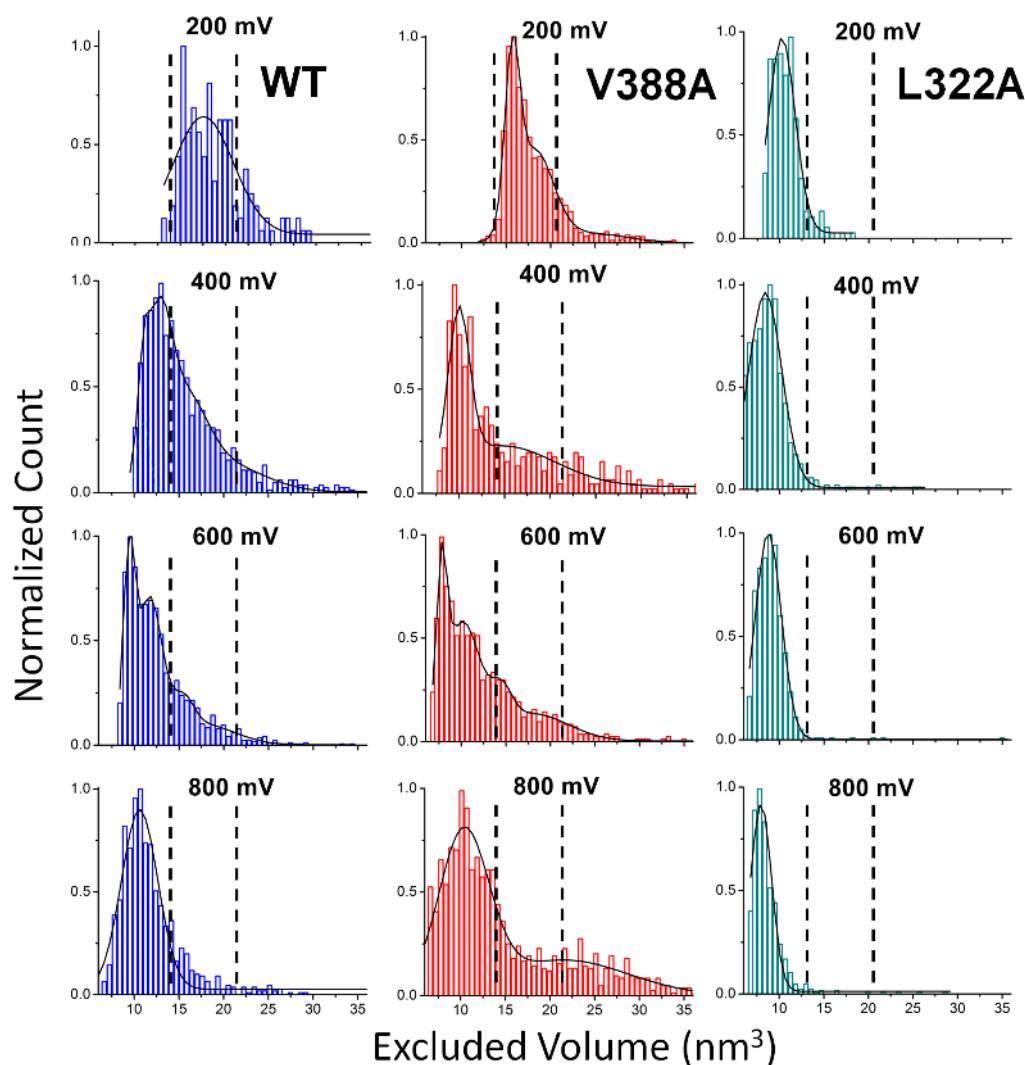


Figure 4 | Excluded volume histograms for all three SAP97 PDZ2 domains (wild type (WT), V388A, and L322A) each at four different applied voltages. The natively folded state was defined as the full width half max of the most stable protein at the lowest applied voltage (200 mV). This criterion was then applied to all other domains at all voltages in order to classify proteins as folded or unfolded. Data was collected with pores 15 ± 2 nm in diameter for each domain: wild type SAP97 PDZ2 ($n_{200\text{mV}} = 202$, $n_{400\text{mV}} = 1005$, $n_{600\text{mV}} = 1474$, $n_{800\text{mV}} = 1006$), V388A ($n_{200\text{mV}} = 1719$, $n_{300\text{mV}} = 703$, $n_{600\text{mV}} = 768$, $n_{800\text{mV}} = 1493$), L322A ($n_{200\text{mV}} = 233$, $n_{400\text{mV}} = 674$, $n_{600\text{mV}} = 607$, $n_{800\text{mV}} = 550$).

Based on the hypothesis that the heterogeneously charged residues within the protein are the cause of protein chain displacement from their native positions, it would be expected that the charges would be separated according to their polarity. It could then be envisioned that regions of the protein that have excess positive charges would be pulled away from those regions with excess negative charge leading to an increase in the effective dipole moment of the protein; therefore further leading to a greater net unfolding force on the molecule. This may play a role in the seemingly strong denaturing force of the electric field that we observe in this study as well as the voltage-dependent nature of antigen-antibody unbinding observed in other studies⁵². If the unfolding forces on the molecule are changing over time spent inside the pore, our current method of analysis is only taking a snapshot of the many states that the protein acquires within the pore. It is also possible that the unfolding fails to produce a fully unfolded molecule due to the transient nature of the proteins residence time within the pore. Future work, particularly with higher bandwidth recordings⁵³, may be able to record intra-event properties that show the unfolding process. Alternatively nanopores can be combined with other single molecule techniques to resolve and study protein folding kinetics using the nanopore structure to create local

regions of high electric field strengths. Ultimately, methods will need to be developed to understand the unfolding in more detail and where within the pore the unfolding occurs as currently this is unknown.

The question of whether a protein can be unfolded inside a nanopore by the electric field has been addressed. The relevant parameters that we believe to be strong predictors of whether a protein will be unfolded include the physico-chemical properties of the protein itself as well as the pore length and geometry (which determines the electric field distribution). Keeping the pore length and geometry the same, we would expect proteins to unfold based on their stability as well as their charge distribution or dipole moment. Protein size will also influence the types of signals that are recorded and the type of unfolding that is produced. For small proteins, in which the contour length is on the same order as the pore length, we would expect to see similar results as those obtained here. However with larger proteins or, alternatively, a thinner membrane, we would expect to see the excluded volume become drastically reduced at higher voltages (greater than that shown here) due to the terminal ends being outside the pore and therefore not contributing to the blockage of ion flow. The pore length, therefore, is a critical parameter and should be tailored to the protein that is being unfolded.

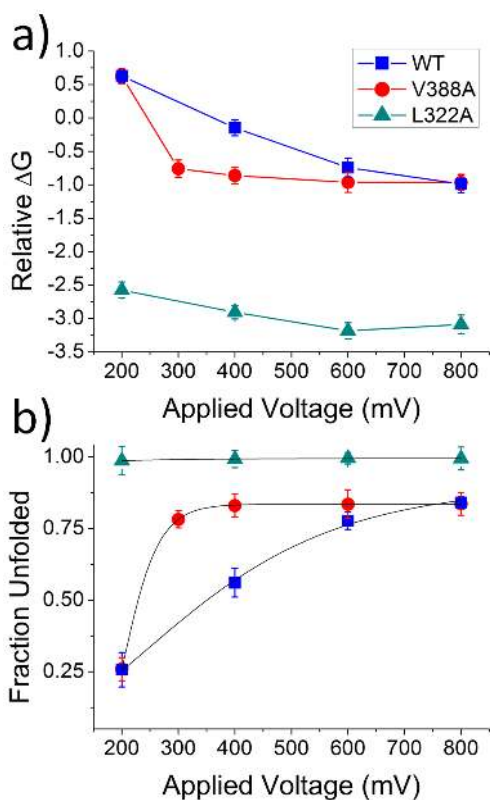


Figure 5 | (a) Relative free energy changes for each protein domain as a function of applied voltage. The free energy change accompanying the conformational unfolding induced by the electric field was calculated using: $\Delta G = -RT \ln(K_{eq})$ where K_{eq} is the fraction of folded molecules. (b) Fraction of unfolded proteins as a function of applied voltage.

The reproducibility of electric field-induced unfolding is largely dependent on the manufacturing of the nanopore devices such that it has minimal dimensional variation and fixed electrode locations to keep the electric field drop within the fluid (however minimal it may be) constant. The wafer-scale production of nanopore chips yields

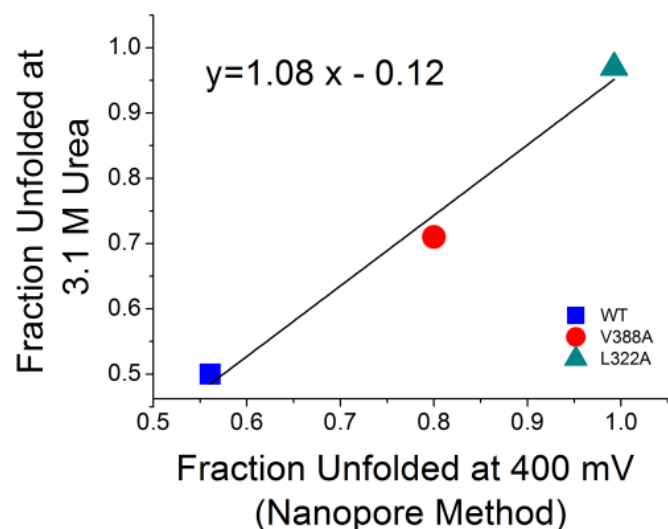


Figure 6 | Fraction unfolded at 3.1 M urea (the concentration where half the WT proteins are unfolded) obtained using fluorimetry versus the fraction unfolded at 400 mV for each domain obtained using nanopores. A slope of 1.08 implies an excellent correlation between the two techniques.

very reproducible membrane thicknesses and electron beam sculpting produces pores with ± 1 nm resolution⁵⁴. Using numerical simulations of the nanopore environment, we found that a deviation of 1 nm in pore diameter led to a rather substantial change in the magnitude of the electric field (13.8% error) while a 5 nm change in pore length led to a 7.5% error. These issues however can easily be circumvented by estimating the pore diameter using the open pore conductance and adjusting the applied voltage prior to adding protein to the nanopore flow cell. Further work on developing nanofluidic environments that make the unfolding more robust will be greatly advantageous for both preventing unwanted changes in protein state or studying the unfolding process of different size proteins.

Methods

Protein expression, purification and equilibrium denaturation. SAP97 PDZ2 was expressed and purified as described^{35,36}. The mutants, L322A and V388A, were made by inverted PCR using the cDNA of SAP97 PDZ2 as template (residues 311–407). The purity of the proteins was checked by SDS-PAGE and their identity by mass spectrometry. Purified SAP97 PDZ2 variants were subjected to urea-induced unfolding experiments. The unfolding transition was monitored using Trp fluorescence (excitation at 280 nm and emission at 340 nm). Data were analyzed using the general equation for solvent denaturation as described^{35,36} to obtain the parameters m_{D-N} (shared in the curve fitting) and $[\text{urea}]_{50\%}$, which were used to calculate ΔG_{D-N} and $\Delta \Delta G_{D-N}$ at 3.1 M urea as reported in Fig. 5. The PDB code for the wild-type SAP97 PDZ2 protein domain is 2X7Z. The sequence is given by the one letter amino acid code as follows: MHHHHHLVPRGSKPVSEKIMEIKLIKPKGLGFSIAGGVGNQHWPGDNDISYVTKIIEGGAHDKGLQIGDKLLAVNNVALEEVTHEEAVTALKNTSDFVYLKVAKPTS. The expressed protein contained an N-terminal His-tag (MHHHHHLVPRGS) in addition to the I342W/C378A mutations. We have shown previously for other PDZ domains that the His-tag does not affect the binding and stability of the PDZ domains^{35,55}. The I342W/C378A mutations served (i) to insert a fluorescent probe (I342W) and (ii) to remove the cysteine residue (C378A), which otherwise might form PDZ dimers via S-S bridges. The other two mutants used in this study were expressed using the same methods. The second and third mutations (L322A and V388A) destabilized the domain due to the deletion of key interactions in the hydrophobic core.

Fabrication. Nanopores were drilled in a 50 nm thick free-standing silicon nitride membrane which was supported on all sides by a silicon chip (5.5×5.5 mm²). Fabrication of this membrane consisted of first depositing a layer of low-stress silicon nitride on a silicon wafer using low pressure chemical vapor deposition (LPCVD) followed by photolithography, deep reactive ion etching (DRIE) and KOH etching to form a 50×50 μm^2 square membrane. Pores were then drilled using a field emission TEM (JEOL 2010F) forming pores with diameters of 15 ± 2 nm.

Single channel recordings. Pore characterization and event recording was accomplished by placing the nanopore between two electrolytic half cells filled with buffered potassium chloride (2 M KCl). The nanopore chip was held in place using a custom built polycarbonate flow cell with PDMS gaskets to assure that the only path of ionic current is through the nanopore. Electrodes (Ag/AgCl) were placed in both chambers and connected to the headstage of a patch clamp amplifier (Axopatch 200B, Molecular Devices Inc.) which allowed the ionic current to be measured at various applied voltages. Signals were recorded at 250 kHz with a lowpass Bessel filter of 10 kHz. Conductance measurements were performed prior to each experiment and were found to be within 5% of each other. A graphical representation of our custom-built flow cell used for all experiments, a TEM image of a 15 nm pore and IV-curve graphs for several pores are shown in the supplementary information.

Data acquisition and analysis. Prior to each experiment, protein solutions were made fresh by diluting the desired protein into buffered KCl for a final protein concentration of 10 nM (diluted in 2 M KCl, 10 mM potassium phosphate buffer, pH 7). After characterization of the pore, protein was injected into one chamber of the flow cell while a constant voltage is applied across the pore. Protein translocation events, defined as transient decreases in current, were detected using a threshold and characterizing features were extracted including event duration and event amplitude. For gold nanoparticle translocation data, the same 15 nm pore was used except with a reduced KCl concentration (0.2 M) to reduce aggregation (0.15 mM triton was also used to reduce aggregation). Particles were obtained through Cytodiagnostics Inc. Event detection was performed using custom Matlab scripts. Residence times were calculated by using the width of the event half-way between the baseline current value and the maximum current drop value. Event statistics (i.e. average current drop value and average translocation time) were obtained by Gaussian and Exponential fits of the data histograms using Origin 8.1.

- Gething, M.-J. & Sambrook, J. Protein folding in the cell. *Nature* **355**, 33–45 (1992).
- Mello, C. C. & Barrick, D. An experimentally determined protein folding energy landscape. *Proc. Natl. Acad. Sci. U.S.A.* **101**, 14102–14107 (2004).



3. Onuchic, J. N., Luthey-Schulten, Z. & Wolynes, P. G. Theory of protein folding: the energy landscape perspective. *Annu. Rev. Phys. Chem.* **48**, 545–600 (1997).
4. Wedemeyer, W. J., Xu, X., Welker, E. & Scheraga, H. A. Conformational propensities of protein folding intermediates: distribution of species in the 1S, 2S, and 3S ensembles of the [C40A,C95A] mutant of bovine pancreatic ribonuclease A. *Biochem.* **41**, 1483–1491 (2002).
5. Daggett, V. & Fersht, A. The present view of the mechanism of protein folding. *Nat. Rev. Mol. Cell Biol.* **4**, 497–502 (2003).
6. Best, R. *et al.* Force mode atomic force microscopy as a tool for protein folding studies. *Anal. Chim. Acta* **479**, 87–105 (2003).
7. Lammert, H., Wolynes, P. G. & Onuchic, J. N. The role of atomic level steric effects and attractive forces in protein folding. *Proteins Struct. Funct. Bioinf.* **80**, 362–373 (2012).
8. Erbaş, A., Horinek, D. & Netz, R. R. Viscous Friction of Hydrogen-Bonded Matter. *J. Am. Chem. Soc.* **134**, 623–630 (2011).
9. Soranno, A. *et al.* Quantifying internal friction in unfolded and intrinsically disordered proteins with single-molecule spectroscopy. *Proc. Natl. Acad. Sci. U.S.A.* **109**, 17800–17806 (2012).
10. Lin, M., Zhang, J., Lu, H.-M., Chen, R. & Liang, J. Constrained proper sampling of conformations of transition state ensemble of protein folding. *J. Chem. Phys.* **134**, 075103–075113 (2011).
11. Naganathan, A. N. & Orozco, M. The protein folding transition-state ensemble from a Go-like model. *Phys. Chem. Chem. Phys.* **13**, 15166–15174 (2011).
12. Kumar, S., Ma, B., Tsai, C.-J., Sinha, N. & Nussinov, R. Folding and binding cascades: Dynamic landscapes and population shifts. *Protein Sci.* **9**, 10–19 (2000).
13. Henzler-Wildman, K. & Kern, D. Dynamic personalities of proteins. *Nature* **450**, 964–972 (2007).
14. Ceconi, C., Shank, E. A., Bustamante, C. & Marqusee, S. Direct observation of the three-state folding of a single protein molecule. *Science* **309**, 2057–2060 (2005).
15. Neuman, K. C. & Nagy, A. Single-molecule force spectroscopy: optical tweezers, magnetic tweezers and atomic force microscopy. *Nat. Methods.* **5**, 491–505 (2008).
16. Rief, M., Gautel, M., Oesterhelt, F., Fernandez, J. M. & Gaub, H. E. Reversible Unfolding of Individual Titin Immunoglobulin Domains by AFM. *Science* **276**, 1109–1112 (1997).
17. Miles, M. N., Ivanov, A. P., Wilson, K. A., Dogan, F., Japrun, D. & Edel, J. B. Single molecule sensing with solid-state nanopores: novel materials, methods, and applications. *Chem. Soc. Rev.* **42**, 15–28 (2012).
18. Korzhnev, D. M., Religa, T. L., Banachewicz, W., Fersht, A. R. & Kay, L. E. A Transient and Low-Populated Protein-Folding Intermediate at Atomic Resolution. *Science* **329**, 1312–1316 (2010).
19. Fologea, D., Ledden, B., McNabb, D. & Li, J. Electrical characterization of protein molecules by a solid-state nanopore. *Appl. Phys. Lett.* **91**, 053901 (2007).
20. Hoogerheide, D. P., Garaj, S. & Golovchenko, J. A. Probing Surface Charge Fluctuations with Solid-State Nanopores. *Phys. Rev. Lett.* **102**, 256804 (2009).
21. Fologea, D., Brandin, E., Uplinger, J., Branton, D. & Li, J. DNA conformation and base number simultaneously determined in a nanopore. *Electrophoresis* **28**, 3186–3192 (2007).
22. Cressiot, B. *et al.* Protein transport through a narrow solid-state nanopore at high voltage: experiments and theory. *ACS Nano* **6**, 6236–6243 (2012).
23. Freedman, K. J. *et al.* Chemical, thermal, and electric field induced unfolding of single protein molecules studied using nanopores. *Anal. Chem.* **83**, 5137–5144 (2011).
24. Merstorf, C. *et al.* Wild type, mutant protein unfolding and phase transition detected by single-nanopore recording. *ACS Chem. Biol.* **7**, 652–658 (2012).
25. Oukhaled, A. *et al.* Dynamics of completely unfolded and native proteins through solid-state nanopores as a function of electric driving force. *ACS Nano* **5**, 3628–3638 (2011).
26. Oukhaled, G. *et al.* Unfolding of proteins and long transient conformations detected by single nanopore recording. *Phys. Rev. Lett.* **98**, 158101 (2007).
27. Payet, L. *et al.* Thermal unfolding of proteins probed at the single molecule level using nanopores. *Analytical Chemistry* **84**, 4071–4076 (2012).
28. Talaga, D. S. & Li, J. Single-molecule protein unfolding in solid state nanopores. *J. Am. Chem. Soc.* **131**, 9287–9297 (2009).
29. Nourry, C., Grant, S. G. N. & Borg, J.-P. PDZ Domain Proteins: Plug and Play! *Sci. STKE* **2003**, re7- (2003).
30. Feng, W. & Zhang, M. Organization and dynamics of PDZ-domain-related supramodules in the postsynaptic density. *Nat. Rev. Neurosci.* **10**, 87–99 (2009).
31. Jemth, P. & Gianni, S. PDZ Domains: Folding and Binding. *Biochem.* **46**, 8701–8708 (2007).
32. Reiners, J., Nagel-Wolfrum, K., Jürgens, K., Märker, T. & Wolfrum, U. Molecular basis of human Usher syndrome: Deciphering the meshes of the Usher protein network provides insights into the pathomechanisms of the Usher disease. *Exp. Eye Res.* **83**, 97–119 (2006).
33. Strauss, K. M. *et al.* Loss of function mutations in the gene encoding Omi/HtrA2 in Parkinson's disease. *Hum. Mol. Genet.* **14**, 2099–2111 (2005).
34. Verpy, E. *et al.* A defect in harmonin, a PDZ domain-containing protein expressed in the inner ear sensory hair cells, underlies Usher syndrome type 1C. *Nat. Genet.* **26**, 51–55 (2000).
35. Chi, C. N. *et al.* A sequential binding mechanism in a PDZ domain. *Biochem.* **48**, 7089–7097 (2009).
36. Haq, S. R. *et al.* The plastic energy landscape of protein folding. *J. Biol. Chem.* **285**, 18051–18059 (2010).
37. Hultqvist, G., Punekar, A., Chi, C. N., Haq, S. R., Engström, Å., Selmer, M., Gianni, S. & Jemth, P. Influence of circular permutation on the folding pathway of a PDZ domain. *PLoS One* **7**, e50055 (2012).
38. Kella, N. & Kinsella, J. E. Enhanced thermodynamic stability of beta-lactoglobulin at low pH. A possible mechanism. *Biochem. J.* **255**, 113–118 (1988).
39. Kosa, T., Maruyama, T. & Otagiri, M. Species differences of serum albumins: II. chemical and thermal stability. *Pharm. Res.* **15**, 449–454 (1998).
40. Grover, N., Naaman, J., Ben-sasson, S. & Doljansky, F. Electrical sizing of particles in suspensions. I. Theory. *Biophys. J.* **9**, 1398–1414 (1969).
41. Yusko, E. *et al.* Controlling protein translocation through nanopores with bio-inspired fluid walls. *Nat. Nanotechnol.* **6**, 253–260 (2011).
42. Jones, J. A., Wilkins, D. K., Smith, L. J. & Dobson, C. M. Characterisation of protein unfolding by NMR diffusion measurements. *J. Biomol. NMR* **10**, 199–203 (1997).
43. D'Aquino, J. A. *et al.* The magnitude of the backbone conformational entropy change in protein folding. *Proteins Struct. Funct. Bioinf.* **25**, 143–156 (1996).
44. Reguera, D. *et al.* Entropic transport: kinetics, scaling, and control mechanisms. *Phys. Rev. Lett.* **96**, 130603 (2006).
45. Pastoriza-Gallego, M. *et al.* Dynamics of unfolded protein transport through an aerolysin pore. *J. Am. Chem. Soc.* **133**, 2923–2931 (2011).
46. Gavina, J. M. A. & Britz-McKibbin, P. Protein unfolding and conformational studies by capillary electrophoresis. *Curr. Anal. Chem.* **3**, 17–31 (2007).
47. Firnkes, M., Pedone, D., Knezevic, J., Döblinger, M. & Rant, U. Electrically facilitated translocations of proteins through silicon nitride nanopores: conjoint and competitive action of diffusion, electrophoresis, and electroosmosis. *Nano Lett.* **10**, 2162–2167 (2010).
48. Sexton, L. T. *et al.* An adsorption-based model for pulse duration in resistive-pulse protein sensing. *J. Am. Chem. Soc.* **132**, 6755–6763 (2010).
49. Movileanu, L. Squeezing a single polypeptide through a nanopore. *Soft Matt.* **4**, 925–931 (2008).
50. Fologea, D., Uplinger, J., Thomas, B., McNabb, D. S. & Li, J. Slowing DNA Translocation in a Solid-State Nanopore. *Nano Lett.* **5**, 1734–1737 (2005).
51. Niedzwiecki, D. J., Grazul, J. & Movileanu, L. Single-molecule observation of protein adsorption onto an inorganic surface. *J. Am. Chem. Soc.* **132**, 10816–10822 (2010).
52. Freedman, K. J., Bastian, A. R., Chaiken, I. & Kim, M. J. Solid-state nanopore detection of protein complexes: applications in healthcare and protein kinetics. *Small* **9**, 750–759 (2013).
53. Rosenstein, J. K., Wanunu, M., Merchant, C. A., Drndic, M. & Shepard, K. L. Integrated nanopore sensing platform with sub-microsecond temporal resolution. *Nat. Methods.* **9**, 487–492 (2012).
54. Storm, A., Chen, J., Ling, X., Zandbergen, H. & Dekker, C. Fabrication of solid-state nanopores with single-nanometre precision. *Nat. Mater.* **2**, 537–540 (2003).
55. Gianni, S. *et al.* Demonstration of long-range interactions in a PDZ domain by NMR, kinetics, and protein engineering. *Struct.* **14**, 1801–1809 (2006).

Acknowledgments

This material is based upon work supported by the National Science Foundation Graduate Research Fellowship under Grant ID No. 2010095296 and the HFSP young investigator award (RGY0075/2009-C). JBE acknowledges the receipt of an European Research Council starting investigator grant and PJ a grant from the Swedish Research Council. Special thanks to Anmiv Prabhu for discussions and help with finite element analysis.

Author contributions

M.J.K., P.J. and J.E. planned and designed experiments. K.J.F. and S.R.H. performed experiments. All authors contributed to writing manuscript.

Additional information

Supplementary information accompanies this paper at <http://www.nature.com/scientificreports>

Competing financial interests: The authors declare no competing financial interests.

License: This work is licensed under a Creative Commons Attribution-NonCommercial-NoDerivs 3.0 Unported License. To view a copy of this license, visit <http://creativecommons.org/licenses/by-nc-nd/3.0/>

How to cite this article: Freedman, K.J., Haq, S.R., Edel, J.B., Jemth, P. & Kim, M.J. Single molecule unfolding and stretching of protein domains inside a solid-state nanopore by electric field. *Sci. Rep.* **3**, 1638; DOI:10.1038/srep01638 (2013).